Title
Effects of partial sleep deprivation on slow waves during non-rapid eye movement sleep: A high density EEG investigation

Journal
Clinical Neurophysiology, 127(2)

ISSN
1388-2457

Authors
Plante, David T
Goldstein, Michael R
Cook, Jesse D
et al.

Publication Date
2016-02-01

DOI
10.1016/j.clinph.2015.10.040

Peer reviewed

HHS Public Access

Author manuscript

Clin Neurophysiol. Author manuscript; available in PMC 2017 February 01.

Published in final edited form as:

Clin Neurophysiol. 2016 February ; 127(2): 1436–1444. doi:10.1016/j.clinph.2015.10.040.

Effects of partial sleep deprivation on slow waves during non-rapid eye movement sleep: a high density EEG investigation

David T. Plante[1], **Michael R. Goldstein**[2], **Jesse D. Cook**[1], **Richard Smith**[1], **Brady A. Riedner**[1], **Meredith E. Rumble**[1], **Lauren Jelenchick**[3], **Andrea Roth**[4], **Giulio Tononi**[1], **Ruth M. Benca**[1], and **Michael J. Peterson**[1]

[1]University of Wisconsin School of Medicine and Public Health, Department of Psychiatry, Madison, WI, USA

[2]Department of Psychology, University of Arizona, Tucson, AZ, USA

[3]University of Minnesota Medical Scientist Training Program Minneapolis, MN, USA

[4]Ferkauf Graduate School of Psychology, Yeshiva University, New York, NY, USA

Abstract

Objective—Changes in slow waves during non-rapid eye movement (NREM) sleep in response to acute total sleep deprivation are well-established measures of sleep homeostasis. This investigation utilized high-density electroencephalography (hdEEG) to examine topographic changes in slow waves during repeated partial sleep deprivation.

Methods—Twenty-four participants underwent a 6-day sleep restriction protocol. Spectral and period-amplitude analyses of sleep hdEEG data were used to examine changes in slow wave energy, count, amplitude, and slope relative to baseline.

Results—Changes in slow wave energy were dependent on the quantity of NREM sleep utilized for analysis, with widespread increases during sleep restriction and recovery when comparing data from the first portion of the sleep period, but restricted to recovery sleep if the entire sleep episode

Corresponding Author: David T. Plante, M.D., Wisconsin Psychiatric Institute and Clinics, 6001 Research Park Blvd., Madison, WI 53719, USA, Tel.: +1-608-262-0130, Fax: +1-608-263-0265, dplante@wisc.edu.

Conflict of interest

Dr. Plante has received royalties from Cambridge University Press. Dr. Riedner is financially supported in part by grants from Merck and Philips Respironics and is involved in several patent applications resulting from research supported by Philips Respironics. Dr. Rumble is supported in part by a grant from Merck. Dr. Tononi has consulted for Sanofi-Aventis and Takeda, and he is currently the David P. White Chair in Sleep Medicine at the University of Wisconsin–Madison, endowed by Phillips Respironics. Dr. Tononi has also received unrelated research support from Phillips Respironics. Dr. Benca has previously served as a consultant for Sanofi-Aventis, is a consultant for Merck and Jazz Pharmaceuticals, and receives grant support from Merck. Dr. Peterson is a member of the medical advisory panel for Otsuka Pharmaceuticals and is a consultant and content author for MedicineNet. All other authors declare they have no conflicts of interest.

Role of Funding Source

Sanofi had no further role in the design of this study, collection of data, analysis and interpretation of data, or writing of the manuscript. Sanofi was provided courtesy review of the manuscript prior to submission, but did not play a role in the decision to submit the report for publication.

was considered. Period-amplitude analysis was less dependent on the quantity of NREM sleep utilized, and demonstrated topographic changes in the count, amplitude, and distribution of slow waves, with frontal increases in slow wave amplitude, numbers of high-amplitude waves, and amplitude/slopes of low amplitude waves resulting from partial sleep deprivation.

Conclusions—Topographic changes in slow waves occur across the course of partial sleep restriction and recovery.

Significance—These results demonstrate a homeostatic response to partial sleep loss in humans.

Keywords

Sleep deprivation; synaptic plasticity; slow wave; electroencephalogram; sleep homeostasis

1. Introduction

Slow waves are a hallmark of non-rapid eye movement (NREM) sleep in humans. These waveforms are reflective of depth of sleep (Blake and Gerard, 1937; Neckelmann and Ursin, 1993), and are an integral component of sleep maintenance, quality, and restoration (Dijk, 2009). Slow waves are homeostatically regulated such that their highest activity occurs during the early portions of sleep, with activity dissipating as the night progresses (Borbely, 1982). Moreover, increases in slow wave activity (SWA) after acute total sleep deprivation are a well-characterized physiological indicator of increased sleep pressure (Achermann et al., 1993; Borbely et al., 1981). These observations have been central to the two-process model of sleep regulation, which posits sleep is regulated by the interaction between a circadian process that oscillates with twenty-four hour periodicity and a homeostatic process that regulates sleep propensity based on the duration of prior wakefulness (Daan et al., 1984).

Although the homeostatic regulation of slow waves in response to a single night of total sleep deprivation has been vital to the study of sleep-related processes and functions, the applicability of homeostatic models in the context of partial sleep restriction occurring over several days is less clear. Animal models that examine EEG spectral power over the course of partial sleep restriction and recovery have demonstrated varied findings. Some investigations have suggested delta power during sleep increases early during the course of partial sleep loss, then attenuates over the longitudinal course of partial sleep deprivation (Kim et al., 2007; Kim et al., 2012; Lancel and Kerkhof, 1989). In addition, paradoxical reductions in NREM delta power relative to baseline during recovery sleep after partial sleep restriction have been described (Kim et al., 2007). Such data suggest that the homeostatic response to acute total sleep deprivation may not generalize to chronic partial sleep loss, and that an allostatic process, rather than (or in addition to) a homeostatic process, may govern sleep regulation during partial sleep deprivation (Kim et al., 2007; Kim et al., 2012). However, it is noteworthy that other investigations have demonstrated increased SWA during sleep across all nights of partial sleep restriction and during recovery sleep, suggesting preserved sleep homeostasis (Leemburg et al., 2010). Notably, seemingly divergent findings in the animal literature may be in part explained by methodological differences among studies regarding the use of total delta energy (i.e. summed delta power)

versus slow wave activity as the measure of sleep homeostatic functioning (Kim et al., 2007; Leemburg et al., 2010).

An important issue to consider when examining spectral changes during partial sleep deprivation and recovery are the methods used to compare sleep episodes that are of different duration. Using SWA can give a skewed perspective when comparing nights with sizeable differences in total sleep time because the longer the sleep episode, the smaller the increase in SWA, and vice-versa (Banks et al., 2010). An alternative to SWA is the use of slow wave energy (SWE), which is the cumulative sum of delta power across each sleep period. However, cumulative slow wave energy is also dependent on total sleep time, since increases in the intensity of slow wave energy can be masked by discrepancies in sleep duration. For example, when examining SWE across repeated restriction to 4-hour sleep opportunities, some prior investigations have demonstrated SWE remains significantly below baseline levels during sleep restriction, with varying SWE during recovery that depends on the duration of recovery sleep time (Banks et al., 2010; Brunner et al., 1990). Conversely, other investigations have demonstrated no change in SWE across 14 days of 4- and 6-hour sleep restriction (Van Dongen et al., 2003). To try to balance the limitations of both SWA and SWE in partial sleep restriction protocols, several investigators have performed analyses across nights utilizing the first ~4 hours of sleep. Using this approach, delta power is increased during both sleep restriction and recovery nights of sleep, suggesting intact homeostatic function during partial sleep deprivation (Akerstedt et al., 2009; Brunner et al., 1990; Brunner et al., 1993). The divergent findings in spectral power that are observed during partial sleep restriction using the first portion of the night or all available sleep data have been more fully described by Akerstedt et al. (2009), demonstrating significant increases in slow wave energy during sleep deprivation nights using the former approach, and reductions or no significant differences using the latter.

In addition to the use of slow wave energy versus activity to evaluate sleep homeostatic function during partial sleep deprivation, there are other factors that may affect findings across studies. The majority of prior investigations have used a limited number of EEG derivations (typically 1–2 central channels) for analysis. Slow waves demonstrate a characteristic topography with increases in frontal channels, and thus studies that utilize limited EEG derivations may fail to find pertinent topographic changes in spectral power across partial sleep restriction (Cajochen et al., 1999; Finelli et al., 2000; Tinguely et al., 2006; Werth et al., 1997). Additionally, alterations in spectral power that occur during sleep restriction are not limited to the delta band, and extend to frequencies in the theta, alpha, and even sigma range, suggesting such changes are not specific to slow waves (Akerstedt et al., 2009). Therefore, the use of period-amplitude analyses may be a more useful technique to examine changes in the incidence and morphology of detected slow waves during partial sleep deprivation. In particular, the use of slow wave slope, which is posited to be a more sensitive marker of sleep pressure, may detect homesostatic alterations in slow waves that cannot be observed using other methods (Riedner et al., 2007; Vyazovskiy et al., 2007).

This study sought to utilize high-density (hd) EEG to evaluate the topographic effects of partial sleep deprivation on slow waves using both spectral and period-amplitude analyses. Based on prior literature, we hypothesized that changes in slow waves would be more

pronounced in frontal EEG derivations and would be more prominently observed when examining data from the initial portions of the sleep period. We also hypothesized that morphologic changes in slow waves (i.e. slope), would prove a more sensitive marker of sleep homeostasis relative to changes in spectral power.

2. Methods

2.1. Participants

Participants were healthy volunteers recruited as part of a larger parent study that examined the effects of psychotropic medications on sleep restriction. Inclusion criteria included age 18–35 years, right-handedness, body mass index (BMI) 19–32kg/m^2, routine bedtime between 21:00 and 01:00 hours, and self-reported typical nightly sleep duration 6.5–8.5 hours. Initial evaluation included the Structured Clinical Interview for DSM-IV Axis I disorders (First et al., 2002), urine drug screen, and urine pregnancy test (for female participants). Exclusion criteria included current or past psychiatric disorder, current or recent major medical or neurological illness, pregnancy, caffeine intake >300mg/day, alcohol intake>3 drinks/day or 8 drinks/week, regular use of nicotine within 6 months of enrollment, use of central nervous system active medications or illicit drugs, night/evening shift work, or travel across ≥3 time zones in the month preceding enrollment. Participants also did not have clinically relevant sleep-related breathing or movement disorders, verified by clinical history and screening polysomnogram. Participants were excluded if they had either subjective or objective excessive daytime sleepiness, defined as Epworth Sleepiness Scale score ≥10 and mean sleep latency <8 minutes on screening multiple sleep latency test, respectively (Johns, 1991; Sullivan and Kushida, 2008). In addition, as part of screening at baseline, potential participants underwent a single night of sleep restriction (4 hour time in bed) to assess vulnerability to sleep loss. Participants who did not show evidence of neurocognitive impairment resulting from sleep restriction on the Digit Symbol Substitution Test or Digit Span Test (defined as decrease pre- to post-sleep restriction of at least one scale score point) were excluded from the study (Wechsler, 1997).

The University of Wisconsin-Madison Health Sciences Institutional Review Board approved this investigation, and all participants provided written informed consent. Participants received financial compensation for their participation in the study.

2.2. Partial Sleep Deprivation

After completion of screening procedures, which additionally included an accommodation night using hdEEG, participants were scheduled to undergo a six-night sleep restriction and recovery protocol. The start of sleep restriction sessions were scheduled so they began approximately 2 weeks (and no less than 7 days) after completion of eligibility screening. Data utilized for these analyses were drawn from the placebo arm of the parent study, and thus participants were free of any psychotropic medications at the time of the study. Prior to in-laboratory sleep restriction protocols, wrist-worn actigraphy was utilized to monitor sleep-wake patterns (Actiwatch, Mini-Mitter, Bend, OR). During the sleep deprivation protocol, participants underwent a baseline (BSL) night in the laboratory, during which sleep hdEEG was recorded during an 8-hour time in bed opportunity (22:00 to 06:00).

Following BSL, participants underwent 4 consecutive nights of sleep restriction during which time in bed was restricted to 5 hours (01:00 to 06:00). The use of constant wake time with delayed bedtime to limit time in bed is consistent with other sleep restriction protocols (Akerstedt et al., 2009; Banks et al., 2010; Van Dongen et al., 2003). HdEEG sleep recordings were collected on the second (SR2) and fourth (SR4) night of sleep restriction. During daytime hours following sleep restriction, participants were administered the psychomotor vigilance task (PVT) at 06:30, 08:30, 10:30; 12:30 and 14:30, and a modified multiple sleep latency test (MSLT) with nap opportunities at 08:00, 10:00, 12:00, and 14:00 (Dinges and Powell, 1985; Littner et al., 2005). The MSLT was modified such that participants were awakened once sleep onset had been confirmed, rather than allowing the nap opportunity to continue to evaluate for sleep-onset REM periods. On the final night of the protocol, participants were allowed a night of recovery sleep (RCV) from 22:00 to 06:00 while hdEEG was recorded. Participants were continuously monitored by study staff throughout the protocol and were not allowed to leave the laboratory unless supervised.

2.3. Sleep EEG

The hdEEG data utilized in this study were collected on four separate nights of sleep (within-subjects design) as described above (BSL, SR2, SR4, and RCV). Sleep data were collected using an integrated recording with 256-channel hdEEG (Electrical Geodesics, Eugene, OR) and parameters for sleep staging (Alice® Sleepware; Philips Respironics, Murrysville, PA). HdEEG signals were collected with a vertex reference and 500 Hz sampling rate. A registered sleep technologist staged all sleep recordings according to standard criteria (Iber et al., 2007) based on 6 EEG channels at approximate 10–20 locations (F3, F4, C3, C4, O1, and O2) referenced to the mastoids, electrooculogram, and sub-mental electromyogram.

2.4. EEG Spectral Analysis

HdEEG signals were first-order high-pass (0.1Hz) filtered and band-pass (0.3–50Hz) filtered in NetStation (Electrical Geodesics, Eugene, OR), then downsampled to 128 Hz, high-pass filtered (2-way least-squares FIR, 1Hz) and re-referenced to the average scalp voltage computed in all channels in MATLAB (MathWorks, Natick, MA). Semi-automatic artifact rejection was applied to remove channels with interrupted contact with the scalp or high-frequency artifact. Spectral analysis of NREM sleep (all N2 and N3 epochs) from 1 to 30Hz was performed for each channel in 6-second epochs (Welch's averaged modified periodogram with a Hamming window; frequency resolution 0.17Hz), which maintained temporal congruence between spectral analysis and 30-second staging epochs (Goldstein et al., 2012; Plante et al., 2012). Slow wave energy (SWE; integrated power 1–4.5Hz totaled over cumulative 6-second epochs of N2/N3 sleep) was the primary measure of spectral power utilized in this study, with other bands examined on an exploratory basis.

2.5. Analysis of Slow Wave Parameters

Slow wave detection and characterization was performed using methods similar to those previously described (Riedner et al., 2007). EEG signals were down-sampled to 128 Hz and band-passed (0.5–4Hz, stop-band 0.1 and 10 Hz) using a Chebyshev Type II filter in MATLAB. Slow waves were defined as negative deflections with 0.25–1.0 second

consecutive zero crossings detected in artifact-free NREM epochs. Analysis was performed on negative deflections because of their increased stability and decreased variability relative to positive deflections. The peak amplitude of each wave between zero crossings was used to calculate mean amplitude (peak amplitude divided by number of detected waves). Similar to prior investigations, an amplitude cut-off of 40 μV was used to define high and low-amplitude waves (Duncan et al., 2012). Slow wave slopes were defined as the amplitude of the most negative peak divided by the time from the previous zero crossing (first-segment slope) or the time until the next zero crossing (second-segment slope).

2.6. Statistical Analysis

Similar to prior investigations (Akerstedt et al., 2009), all analyses were carried out for the entire sleep episode, as well as the first 3.7 hours of sleep, which was the minimum sleep duration among the 96 total recordings. Sleep staging, PVT lapses, and mean sleep onset during modified MSLT were analyzed using repeated measures analysis of variance (ANOVA), with the primary comparisons of interest being baseline versus SR2, SR4, and RCV, respectively. To minimize the likelihood of spurious results from multiple comparisons, global (average of 173 channels) slow wave energy, count, amplitude, and slopes were also subject to repeated measures ANOVA. Topographic analysis of these measures were subsequently investigated for F-ratios corresponding to $p<0.05$ derived from global data. Topographic comparisons of slow wave data for SR2, SR4, and RCV compared to baseline were performed using channel-by-channel paired t-tests. Statistical non-parametric mapping with suprathreshold cluster testing was utilized to correct for multiple comparisons of topographic data using a t-value threshold corresponding to alpha=0.05 for the uncorrected comparisons (Nichols and Holmes, 2002). Missing data for an isolated channel was interpolated in MATLAB using the average of surrounding channels in order to maintain maximal degrees of freedom without altering the mean signal of the group. Statistical analyses were performed using MATLAB and JMP Version 11.0 (SAS Institute Inc., Cary, NC).

3. Results

3.1. Participants, Sleep Staging, & Neurobehavioral Measures

Data from twenty-four participants (14 female; 10 male), mean age 23.3±4.0 (range 18–29) years who completed the sleep restriction protocol were utilized in these analyses. Actigraphy demonstrated mean time in bed of 7.76±0.66 hours (average bedtime 00:44 and wake time 08:45) and sleep duration of 6.77±0.73 hours prior to in-laboratory testing. Sleep staging variables are presented in Table 1. For the full sleep episode, total sleep time (TST), N1,2,3 time, sleep onset latency (SOL), wake after sleep onset (WASO), sleep efficiency (SE), rapid eye movement (REM) time and REM latency all varied significantly across sleep restriction and recovery. As anticipated, TST decreased during SR2 and SR4, but increased during RCV, relative to baseline. N2 time demonstrated a similar pattern to TST. Sleep efficiency increased on all nights relative to baseline, with corresponding decreases in SOL and WASO. Additionally, lighter stages of sleep (i.e. N1) decreased during sleep restriction and recovery nights, with increases in deeper (i.e. N3) sleep in SR4 and RCV relative to baseline. REM sleep time initially decreased from baseline to SR2, but significantly

rebounded above baseline during RCV, consistent with prior reports (Newman et al., 2009; Rechtschaffen et al., 1999). Latency to REM sleep significantly decreased across all conditions relative to baseline.

When only the first 3.7 hours of sleep were examined, changes across sleep restriction and recovery were significant for all variables except N2. Patterns of change of traditional sleep architecture variables were similar to those examined using the entire night of sleep (Table 1).

Mean number of PVT lapses varied across partial sleep restriction ($F_{2,45}$=3.8; p=0.030), with increases relative to baseline for SR2 (p=0.023) and SR4 (0.036). Additionally, mean sleep latency on modified MSLT varied across sleep restriction ($F_{2,46}$=21.9; p<0.0001), with significant reductions relative to baseline for SR2 and SR4 days (p<0.0001 for both comparisons).

3.2. Slow Wave Energy, Amplitude, Count, and Slope

Global SWE (1–4.5Hz; average of 173 channels) varied across partial sleep restriction using both all NREM data and the first 3.7 hours of sleep (Table 1). Consistent with prior investigations (Cajochen et al., 1999; Finelli et al., 2000; Tinguely et al., 2006; Werth et al., 1997), SWE predominantly occurred in frontal regions across all conditions (Figure 1). Using all night data, SWE (1–4.5Hz) did not demonstrate significant topographic changes from baseline to SR2 or SR4, but significantly increased broadly across the scalp during RCV. When analyses were limited to the first 3.7 hours of sleep, SWE increased widely across the scalp in SR2, SR4, and RCV relative to baseline (Figure 1). Notably, the t-value maps associated with changes in SWE during RCV did not demonstrate a consistent frontal predominance.

Results of global period amplitude analyses are presented in Table 2. When all detected slow waves were examined in aggregate, there were significant effects across conditions during all NREM and the first 3.7 hours of sleep for mean amplitude and count, but not slopes of these waveforms. The amplitude of all detected slow waves demonstrated prominent topographic increases in frontal regions relative to baseline in SR2 and SR4 using all night data and data from the first 3.7 hours of sleep (Figure 2). Frontal increases in amplitude for RCV relative to baseline were significant only when examining the first portion of the sleep period, however, similar frontal topographies were observed for all night data (Figure 2).

Using all night data, total slow wave count did not differ from baseline for SR2 or SR4, but widely increased across the scalp during RCV, most prominent in frontal regions (Figure 3A). Aggregate slow wave counts increased relative to baseline during the first 3.7 hours of sleep across the scalp, with increases that were most prominent in lateral centro-parietal channels (Figure 3A). The observed changes in aggregate slow wave amplitude and count supported the further stratification of detected slow waves into high (≥40 μV) and low (<40 μV) amplitude waves (Duncan et al., 2012). Significant changes in global counts of high and low amplitude waves were observed across conditions using waves detected across all NREM sleep and the first 3.7 hours of sleep (Table 2). Topographically, high amplitude waves demonstrated increased counts in frontal regions relative to baseline that were

significant during SR4 and RCV using all night data, as well as SR2, SR4, and RCV using data from the initial 3.7 hours of sleep (Figure 3B). In parallel, the number of low-amplitude slow waves decreased most prominently in frontal regions from baseline to SR2 and SR4 using all night data (Figure 3C). During RCV, the counts of low amplitude slow waves increased across the scalp, but this increase was less pronounced in frontal regions; the converse topography of high-amplitude waves during recovery (Figure 3C). When only the first 3.7 hours of sleep were examined, increases in counts of low amplitude slow waves were observed outside of frontal areas in SR2, SR4, and RCV relative to baseline. These changes in the distribution of slow wave counts by amplitude, with increases in high amplitude and reductions in low amplitude waves, that were more prominent in frontal derivations, are illustrated in Supplementary Figure S1 for visualization purposes.

Although there were no significant global differences in the morphology (amplitude or slope) of high-amplitude slow waves across conditions, there were significant changes in these measures observed for low amplitude waves (Table 2). Topographical analyses demonstrated frontal increases relative to baseline in the amplitude of waves <40 μV for SR2, SR4, and RCV using data from the entire night as well as the first 3.7 hours of sleep (Figure 4A). The shift in the amplitude distribution of these waves, that was more prominent in frontal derivations, is illustrated in Supplementary Figure S2 for visualization purposes. In addition, increases in both first-and second-segment slopes became increasingly frontally predominant from baseline to SR2 and SR4 using data from the entire night and the first 3.7 hours of sleep (Figure 4B,C). Frontal increases in slopes of low amplitude waves were observed during RCV sleep, that were statistically significant using data from the first 3.7 hours of sleep (Figure 4B,C).

3.3. Additional exploratory analyses

Because global (average 173 channels) data that were utilized in ANOVA could theoretically miss small but pertinent topographic differences across conditions, changes in high-amplitude slow wave morphology (amplitude, slope) were further examined on an exploratory basis. However, these analyses demonstrated no significant topographic changes in these variables across conditions. In addition, differences in slow wave energy, count, and morphology between SR2 and SR4 were examined on an exploratory basis, with no significant topographic differences observed for these comparisons.

Also, because changes in spectral energy across sleep restriction and recovery may not be confined to SWE, we also examined broader changes from 1–30Hz. To determine bands for which global spectral energy changed significantly relative to baseline, the percentage change from baseline with 95% confidence interval (CI) was derived for each 0.17Hz frequency bin. Similar to prior investigations (Akerstedt et al., 2009), the CI was interpreted as a significance test for change in spectral energy from baseline (Supplementary Figure S3). Using all night data, there were significant increases from 1–1.83Hz and 1–2.17Hz and decreases from 10.83–30Hz and 10.33–30Hz for SR2 and SR4 relative to baseline respectively. On recovery sleep, all night data demonstrated significant increases from 1–14.67Hz relative to baseline. When examining global spectral energy during the first 3.7 hours of sleep, there were significant increases relative to baseline observed from 1–11.5

Hz, 1–11.33Hz and 1–11.67 Hz for SR2, SR4, and RCV respectively (Supplementary Figure S3). Given these results, we subsequently examined topographic changes in spectral power from 1–2Hz and broad frequency range (1–14.67Hz). Topographic data were very similar to those reported for SWE (1–4.5Hz), with an additional statistically significant left frontal cluster of increased 1–2Hz energy in SR4 relative to baseline using all night data (Supplementary Figure S4).

4. Discussion

Our results demonstrate that slow wave energy, amplitude, count, and slope change across the course of partial sleep deprivation and recovery, reflecting a homeostatic response during repeated partial sleep loss in humans. Our findings are congruent with prior observations that changes in spectral power across sleep restriction are dependent on the sample of NREM sleep utilized (i.e. the first portion of the night versus the entire sleep period) and that alterations in spectral power during chronic partial sleep loss extend well beyond the delta band (Akerstedt et al., 2009).

Importantly, several dynamic changes in the count, amplitude, and slope of slow waves during partial sleep deprivation were observed that varied depending on brain topography and were less dependent on the quantity of NREM sleep examined relative to spectral data. First, there was a frontal increase in aggregate slow wave amplitude, resulting from a relative increase in the number of high amplitude slow waves and concurrent reduction in the count of low amplitude slow waves. It is noteworthy that the number of high-amplitude slow waves in frontal brain regions increased across sleep restriction, such that statistically significant changes were observed by SR4 using all night data, despite significantly less total sleep time. The size and slopes of high-amplitude slow waves remained unchanged during sleep restriction, suggesting that there may be a ceiling effect on the morphology of high-amplitude waves, which is compensated for by an increase in their count rather than morphology. Because increases in counts of high amplitude waves have been similarly observed in total sleep deprivation paradigms (Bersagliere and Achermann, 2010), our results are consistent with a homeostatic response to partial sleep deprivation.

In addition to changes observed in high-amplitude waves, there were also prominent topographic changes in the amplitude and slope of low amplitude waves observed across sleep restriction and recovery, such that they had higher (on average) amplitudes and steeper slopes during sleep restriction and recovery, again more prominently observed in frontal brain regions. Notably, changes in the amplitude and slope of low amplitude slow waves were observed in SR2 and SR4, regardless of the quantity of NREM sleep analyzed, suggesting these measures may be particularly sensitive to homeostatic changes that are occurring during partial sleep deprivation (Riedner et al., 2007; Vyazovskiy et al., 2007).

Our methods, which utilize scalp-level EEG recordings, are not able to directly measure changes at the neuronal level that are responsible for the alterations in slow waves we observed during sleep restriction and recovery. However, recent experimental data supports the hypothesis that slow waves are related to synaptic strength (Huber et al., 2004; Huber et al., 2006; Huber et al., 2007; Riedner et al., 2007; Tononi and Cirelli, 2006; Tononi and

Cirelli, 2014; Vyazovskiy et al., 2007; Vyazovskiy et al., 2008). This model posits that plastic processes that occur during waking result in increases in synaptic efficacy, with subsequent down-selection during sleep that is reflected in homeostatic changes in slow waves. In this context, our results would be consistent with cumulative changes in slow waves across sleep restriction that result from repeated inadequate synaptic downscaling from progressive sleep curtailment. Notably, recent investigations have demonstrated that high cognitive workload induced by a visual task, when combined with chronic sleep restriction, resulted in changes in slow wave energy that were restricted to occipital derivations (Goel et al., 2014). Thus, further work that evaluates how specific cognitive tasks during sleep restriction induce local changes in the amplitude and slopes of slow waves may be a fruitful avenue of future research.

There are other limitations to this study that merit discussion. First, we did not assess genetic polymorphisms that have been linked to differential neurobehavioral and EEG responses to sleep restriction in our study participants (Goel et al., 2009; Goel et al., 2010; Goel et al., 2011). However, all participants did demonstrate some degree of neurobehavioral impairment from a night of sleep restriction during the screening process, decreasing the likelihood that participants had a genotype that would impart resistance to the effects of sleep curtailment. Second, we were not able to assess changes in waking EEG, such as increases in theta waves/activity, which have been demonstrated to reflect homeostatic processes in other sleep restriction paradigms (Ehlen et al., 2013; Leemburg et al., 2010) Third, partial sleep deprivation studies are inherently more variable in design relative to total sleep deprivation protocols because of variations in the amount of nightly sleep restriction and the chronicity of sleep curtailment investigated. Our findings may have varied had we limited participants to a different quantity of time in bed (e.g. 4 instead of 5 hours), extended the paradigm over a greater number of consecutive days, or allowed repeated nights for recovery sleep. Thus, methodological differences between other sleep restriction protocols must be considered when comparing our findings to other investigations.

Despite these limitations, the results of our study that utilized high-density EEG during sleep, as well as both spectral and period-amplitude analyses to characterize slow waves, extends the previous literature on the homeostatic response in humans during partial sleep deprivation. Specifically, we found topographic alterations in slow wave count and morphology that vary by the amplitude of the waveform. These changes occurred across the course of sleep restriction and recovery, suggesting sleep homeostasis was maintained during chronic sleep restriction. Future research that combines spectral and period-amplitude analysis to examine local use-dependent changes in slow waves during sleep restriction are likely to provide further insights into the processes that underlie homeostatic sleep regulation in humans.

Supplementary Material

Refer to Web version on PubMed Central for supplementary material.

Acknowledgments

This research was funded by an investigator-initiated grant by Sanofi, U.S., Inc. (EPLIV-C-03411) to Dr. Peterson. Dr. Plante is supported by grants from NIMH (K23MH099234), the American Sleep Medicine Foundation (Junior Faculty Award: 76-JF-12), and The Brain and Behavior Research Foundation (NARSAD Young Investigator Award: 19193).

References

Achermann P, Dijk DJ, Brunner DP, Borbely AA. A model of human sleep homeostasis based on EEG slow-wave activity: quantitative comparison of data and simulations. Brain Res Bull. 1993; 31:97–113. [PubMed: 8453498]

Akerstedt T, Kecklund G, Ingre M, Lekander M, Axelsson J. Sleep homeostasis during repeated sleep restriction and recovery: support from EEG dynamics. Sleep. 2009; 32:217–22. [PubMed: 19238809]

Banks S, Van Dongen HP, Maislin G, Dinges DF. Neurobehavioral dynamics following chronic sleep restriction: dose-response effects of one night for recovery. Sleep. 2010; 33:1013–26. [PubMed: 20815182]

Bersagliere A, Achermann P. Slow oscillations in human non-rapid eye movement sleep electroencephalogram: effects of increased sleep pressure. J Sleep Res. 2010; 19:228–37. [PubMed: 19845847]

Blake H, Gerard RW. Brain potentials during sleep. Am J Physiol. 1937; 119:692– 703.

Borbely AA, Baumann F, Brandeis D, Strauch I, Lehmann D. Sleep deprivation: effect on sleep stages and EEG power density in man. Electroencephalogr Clin Neurophysiol. 1981; 51:483–495. [PubMed: 6165548]

Borbely AA. A two process model of sleep regulation. Hum Neurobiol. 1982; 1:195– 204. [PubMed: 7185792]

Brunner DP, Dijk DJ, Tobler I, Borbély AA. Effect of partial sleep deprivation on sleep stages and EEG power spectra: evidence for non-REM and REM sleep homeostasis. Electroencephalogr Clin Neurophysiol. 1990; 75:492– 9. [PubMed: 1693894]

Brunner DP, Dijk DJ, Borbély AA. Repeated partial sleep deprivation progressively changes in EEG during sleep and wakefulness. Sleep. 1993; 16:100– 13. [PubMed: 8446828]

Cajochen C, Foy R, Dijk DJ. Frontal predominance of a relative increase in sleep delta and theta EEG activity after sleep loss in humans. Sleep Res Online. 1999; 2:65–69. [PubMed: 11382884]

Daan S, Beersma DG, Borbély AA. Timing of human sleep: recovery process gated by a circadian pacemaker. Am J Physiol. 1984; 246:R161–83. [PubMed: 6696142]

Dijk DJ. Regulation and functional correlates of slow wave sleep. J Clin Sleep Med. 2009; 5:S6–15. [PubMed: 19998869]

Dinges DF, Powell JW. Microcomputer analysis of performance on a portable, simple visual RT task sustained operations. Behav Res Meth Instrum Comput. 1985; 17:652–655.

Duncan WC, Sarasso S, Ferrarelli F, Selter J, Riedner BA, Hejazi NS, Yuan P, Brutsche N, Manji HK, Tononi G, Zarate CA. Concomitant BDNF and sleep slow wave changes indicate ketamine-induced plasticity in major depressive disorder. Int J Neuropsychopharmacol. 2013; 16:301–311. [PubMed: 22676966]

Ehlen JC, Jefferson F, Brager AJ, Benveniste M, Paul KN. Period-amplitude analysis reveals wake-dependent changes in the electroencephalogram during sleep deprivation. Sleep. 2013; 36:1723–35. [PubMed: 24179307]

Finelli LA, Baumann H, Borbely AA, Achermann P. Dual electroencephalogram markers of human sleep homeostasis: correlation between theta activity in waking and slow-wave activity in sleep. Neuroscience. 2000; 101:523–529. [PubMed: 11113301]

First, M.; Spitzer, R.; Gibbon, M.; Williams, J. Structured clinical interview for DSM-IV-TR axis I disorders, research version, non-patient edition (SCID-I/NP). Biometrics Research, New York State Psychiatric Institute; New York: 2002.

Goel N, Banks S, Mignot E, Dinges DF. PER3 polymorphism predicts cumulative sleep homeostatic but not neurobehavioral changes to chronic partial sleep deprivation. PLoS One. 2009; 4:e5874. [PubMed: 19516903]

Goel N, Banks S, Mignot E, Dinges DF. DQB1*0602 predicts interindividual differences in physiologic sleep, sleepiness, and fatigue. Neurology. 2010; 75:1509– 19. [PubMed: 20975052]

Goel N, Banks S, Lin L, Mignot E, Dinges DF. Catechol-O-methyltransferase Val158Met polymorphism associates with individual differences in sleep physiologic responses to chronic sleep loss. PLoS One. 2011; 6:e29283. [PubMed: 22216231]

Goel N, Abe T, Braun ME, Dinges DF. Cognitive workload and sleep restriction interact to influence sleep homeostatic responses. Sleep. 2014; 37:1745–56. [PubMed: 25364070]

Goldstein MR, Plante DT, Hulse BK, Sarasso S, Landsness EC, Tononi G, Benca RM. Overnight changes in waking auditory evoked potential amplitude reflect altered sleep homeostasis in major depression. Acta Psychiatr Scand. 2012; 125:468–77. [PubMed: 22097901]

Huber R, Ghilardi MF, Massimini M, Tononi G. Local sleep and learning. Nature. 2004; 430:78–81. [PubMed: 15184907]

Huber R, Ghilardi MF, Massimini M, Ferrarelli F, Riedner BA, Peterson MJ, Tononi G. Arm immobilization causes cortical plastic changes and locally decreases sleep slow wave activity. Nat Neurosci. 2006; 9:1169–1176. [PubMed: 16936722]

Huber R, Esser SK, Ferrarelli F, Massimini M, Peterson MJ, Tononi G. TMS-induced cortical potentiation during wakefulness locally increases slow wave activity during sleep. PLoS One. 2007; 2:e276. [PubMed: 17342210]

Iber, C.; Ancoli-Israel, S.; Chesson, AL.; Quan, SF. The AASM Manual for the Scoring of Sleep and Associated Events: Rules, Terminology, and Technical Specifications. 1. American Academy of Sleep Medicine; Westchester, Illinois: 2007.

Johns MW. A new method for measuring daytime sleepiness: the Epworth sleepiness scale. Sleep. 1991; 14:540–545. [PubMed: 1798888]

Kim Y, Laposky AD, Bergmann BM, Turek FW. Repeated sleep restriction in rats leads to homeostatic and allostatic responses during recovery sleep. Proc Natl Acad Sci USA. 2007; 104:10697–702. [PubMed: 17548824]

Kim Y, Bolortuya Y, Chen L, Basheer R, McCarley RW, Strecker RE. Decoupling of sleepiness from sleep time and intensity during chronic sleep restriction: evidence for a role of the adenosine system. Sleep. 2012; 35:861–9. [PubMed: 22654205]

Lancel M, Kerkhof GA. Effects of repeated sleep deprivation in the dark- or light-period on sleep in rats. Physiol Behav. 1989; 45:289–97. [PubMed: 2756014]

Leemburg S, Vyazovskiy VV, Olcese U, Bassetti CL, Tononi G, Cirelli C. Sleep homeostasis in the rat is preserved during chronic sleep restriction. Proc Natl Acad Sci USA. 2010; 107:15939–15944. [PubMed: 20696898]

Littner MR, Kushida C, Wise M, Davila DG, Morgenthaler T, Lee-Chiong T, Hirshkowitz M, Daniel LL, Bailey D, Berry RB, Kapen S, Kramer M. Practice parameters for clinical use of the multiple sleep latency test and the maintenance of wakefulness test. Sleep. 2005; 28:113–21. [PubMed: 15700727]

Neckelmann D, Ursin R. Sleep stages and EEG power spectrum in relation to acoustical stimulus arousal threshold in the rat. Sleep. 1993; 16:467–77. [PubMed: 8378687]

Newman SM, Paletz EM, Obermeyer WH, Benca RM. Sleep deprivation in pigeons and rats using motion detection. Sleep. 2009; 32:1299–312. [PubMed: 19848359]

Nichols TE, Holmes AP. Nonparametric permutation tests for functional neuroimaging: a primer with examples. Hum Brain Mapp. 2002; 15:1–25. [PubMed: 11747097]

Plante DT, Landsness EC, Peterson MJ, Goldstein MR, Riedner BA, Wanger T, Guokas JJ, Tononi G, Benca RM. Sex-related differences in sleep slow wave activity in major depressive disorder: a high-density EEG investigation. BMC Psychiatry. 2012; 12:146. [PubMed: 22989072]

Rechtschaffen A, Bergmann BM, Gilliland MA, Bauer K. Effects of method, duration, and sleep stage on rebounds from sleep deprivation in the rat. Sleep. 1999; 22:11–31. [PubMed: 9989363]

Riedner BA, Vyazovskiy VV, Huber R, Massimini M, Esser S, Murphy M, Tononi G. Sleep homeostasis and cortical synchronization: III. A highdensity EEG study of sleep slow waves in humans. Sleep. 2007; 30:1643–57. [PubMed: 18246974]

Sullivan SS, Kushida CA. Multiple sleep latency test and maintenance of wakefulness test. Chest. 2008; 134:854–861. [PubMed: 18842919]

Tinguely G, Finelli LA, Landolt HP, Borbely AA, Achermann P. Functional EEG topography in sleep and waking: state-dependent and state-independent features. Neuroimage. 2006; 32:283–292. [PubMed: 16650779]

Tononi G, Cirelli C. Sleep function and synaptic homeostasis. Sleep Med Rev. 2006; 10:49–62. [PubMed: 16376591]

Tononi G, Cirelli C. Sleep and the price of plasticity: from synaptic and cellular homeostasis to memory consolidation and integration. Neuron. 2014; 81:12–34. [PubMed: 24411729]

Van Dongen HP, Maislin G, Mullington JM, Dinges DF. The cumulative cost of additional wakefulness: dose-response effects on neurobehavioral functions and sleep physiology from chronic sleep restriction and total sleep deprivation. Sleep. 2003; 26:117–26. [PubMed: 12683469]

Vyazovskiy VV, Riedner BA, Cirelli C, Tononi G. Sleep homeostasis and cortical synchronization: II. A local field potential study of sleep slow waves in the rat. Sleep. 2007; 30:1631–42. [PubMed: 18246973]

Vyazovskiy VV, Cirelli C, Pfister-Genskow M, Faraguna U, Tononi G. Molecular and electrophysiological evidence for net synaptic potentiation in wake and depression in sleep. Nat Neurosci. 2008; 11:200–8. [PubMed: 18204445]

Wechsler, D. Wechsler Adult Intelligence Scale. 3. The Psychological Corporation; San Antonio, TX: 1997.

Werth E, Achermann P, Borbely AA. Fronto-occipital EEG power gradients in human sleep. J Sleep Res. 1997; 6:102–112. [PubMed: 9377529]

Highlights

- It is not clear whether homeostatic regulation of slow waves occurs over repeated nights of partial sleep restriction.
- High-density EEG sleep recordings demonstrate dynamic changes during partial sleep deprivation and recovery that vary depending on cortical topography.
- These results confirm a homeostatic response to partial sleep loss in humans.

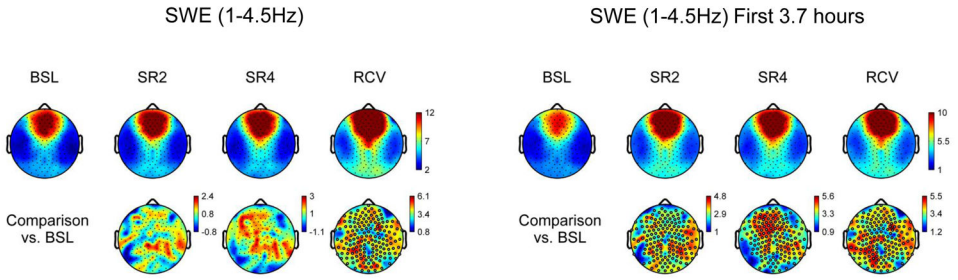

Figure 1.

Topographic slow wave energy (SWE; 1–4.5Hz) during NREM sleep for the full sleep episode (left columns) and the first 3.7 hours of sleep (right column). Values displayed $x10^4$. Lower row displays t-values for channel-by-channel paired t-tests for sleep restriction and recovery conditions versus baseline (BSL). Note plotted t-value ranges differ for each displayed comparison for visualization purposes. SR2/4=Second and fourth night of sleep restriction; RCV=recovery night. White dots denote significant channels after statistical non-parametric mapping with suprathreshold cluster test.

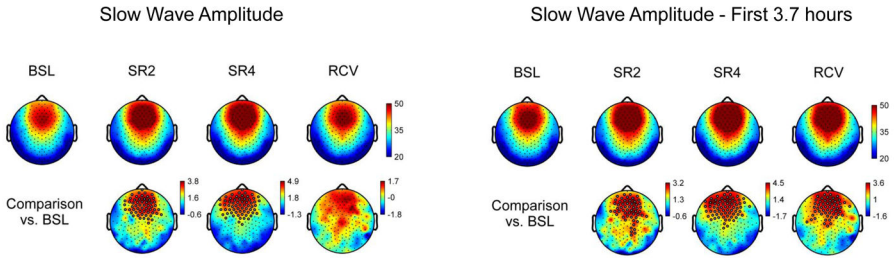

Figure 2.

Topographic amplitude (μV) of all detected slow waves during NREM sleep for the full sleep episode (left column) and the first 3.7 hours of sleep (right column). Lower row displays t-values for channel-by-channel paired t-tests for sleep restriction and recovery conditions versus baseline (BSL). Note plotted t-value ranges differ for each displayed comparison for visualization purposes. SR2/4=Second and fourth night of sleep restriction; RCV=recovery night. White dots denote significant channels after statistical non-parametric mapping with suprathreshold cluster test.

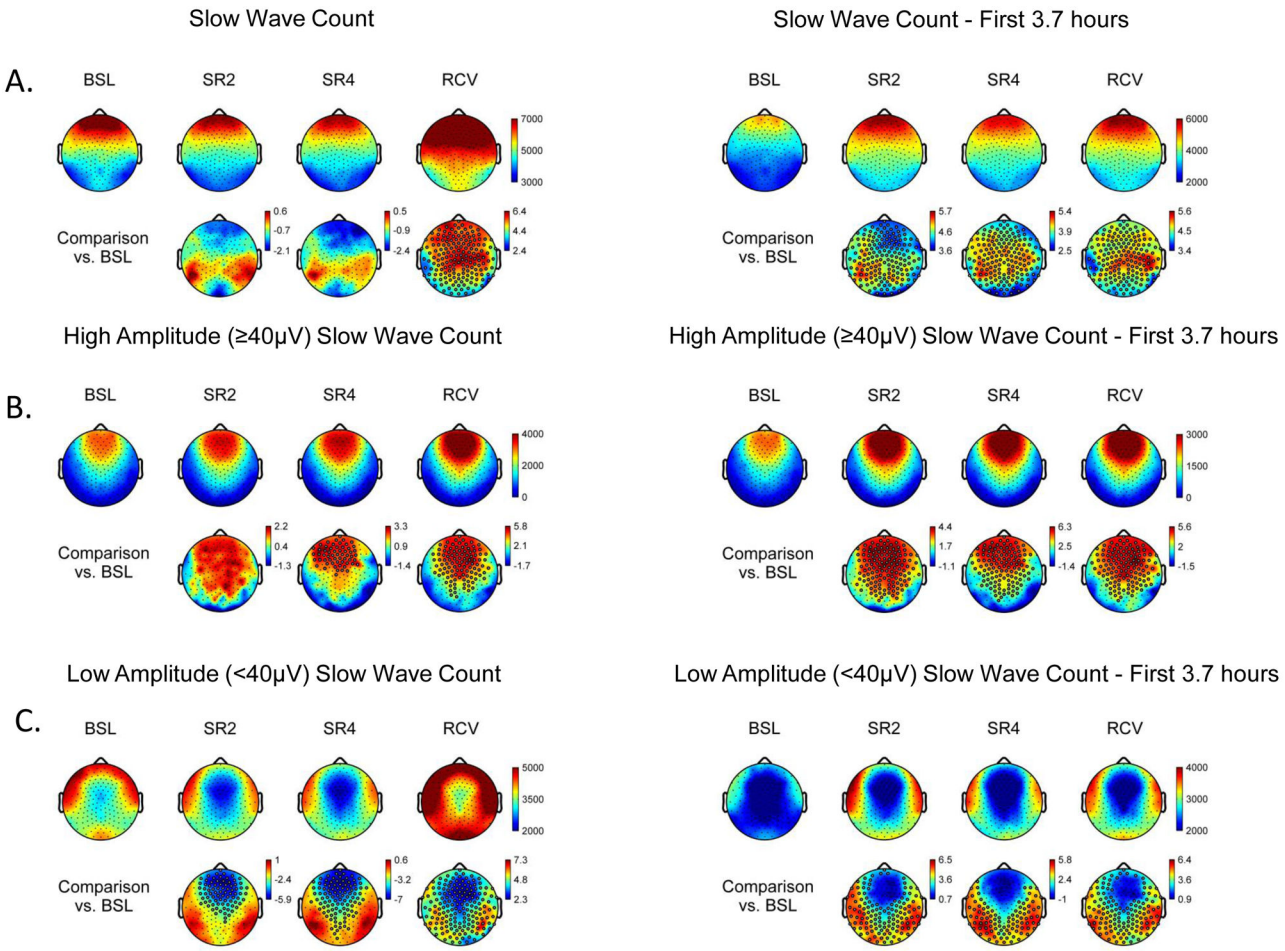

Figure 3.

Topographic slow wave count for A) all detected slow waves, B) high amplitude (≥40 μV) and C) low amplitude (<40 μV) slow waves detected during NREM sleep for the full sleep episode (left column) and the first 3.7 hours of sleep (right column). Lower rows display t-values for channel-by-channel paired t-tests for sleep restriction and recovery conditions versus baseline (BSL). Note plotted t-value ranges differ for each displayed comparison for visualization purposes. SR2/4=Second and fourth night of sleep restriction; RCV=recovery night. White dots denote significant channels after statistical non-parametric mapping with suprathreshold cluster test.

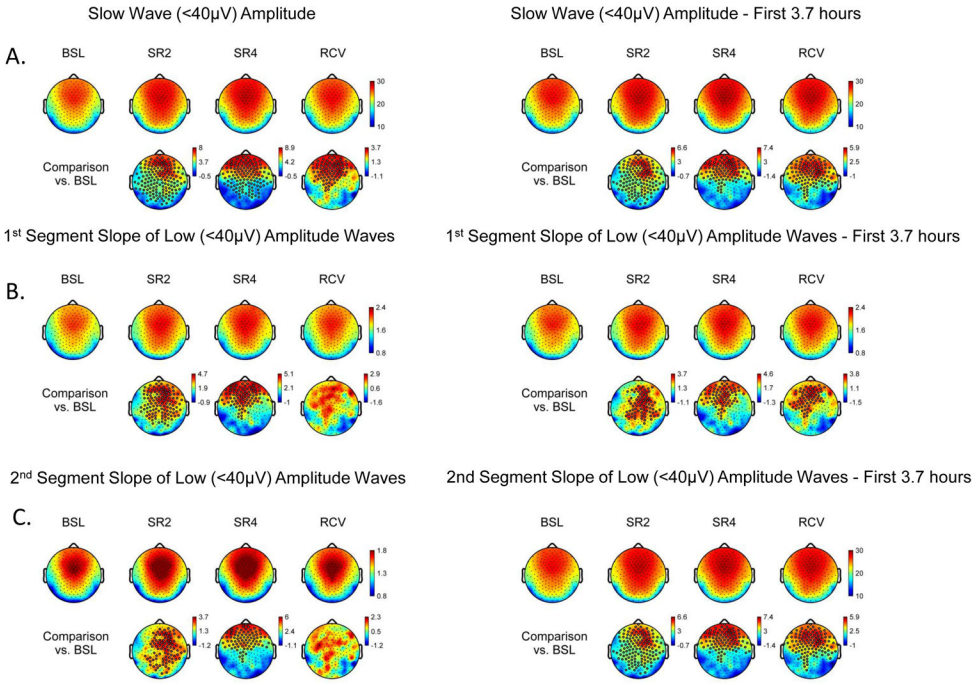

Figure 4.

Topographic A) mean amplitude (μV) B) 1st segment slope (μV/sample), and C) 2nd segment slope (μV/sample) for low amplitude (<40 μV) slow waves detected during NREM sleep for the full sleep episode (left column) and the first 3.7 hours of sleep (right column). Lower rows display t-values for channel-by-channel paired t-tests for sleep restriction and recovery conditions versus baseline (BSL). Note plotted t-value ranges differ for each displayed comparison for visualization purposes. SR2/4=Second and fourth night of sleep restriction; RCV=recovery night. White dots denote significant channels after statistical non-parametric mapping with suprathreshold cluster test.

Clin Neurophysiol. Author manuscript; available in PMC 2017 February 01.

Table 1

Sleep staging and global spectral data.

Full Sleep Episode						
Parameter	**BSL**	**SR2**	**SR4**	**RCV**	**F-ratio**	**p-value**
TST (min)	412.6 (43.6)	284.5 (11.6)***	291.6 (20.2)***	455.1 (30.2)***	210.4	<0.0001
WASO (min)	43.2 (33.6)	9.5 (6.7)***	12.0 (19.8)***	20.4 (13.4)**	14.6	<0.0001
SE (%)	87.8 (8.3)	95.4 (3.2)***	95.4 (5.9)***	94.4 (3.3)***	10.9	<0.0001
SOL (min)	14.9 (15.7)	4.4 (5.9)**	2.3 (2.1)***	6.5 (6.1)*	9.1	<0.0001
N1 (min)	47.3 (31.6)	17.6 (14.5)***	13.3 (7.4)***	21.1 (11.4)***	19.1	<0.0001
N2 (min)	248.9 (45.5)	155.9 (36.0)***	149.1 (24.9)***	255.8 (42.4)	60.1	<0.0001
N3 (min)	47.3 (26.3)	59.8 (28.1)	65.2 (23.0)**	78.1 (26.9)***	7.8	0.0001
REM (min)	69.4 (30.5)	51.4 (19.7)*	64.3 (20.2)	100.4 (31.6)**	20.5	<0.0001
REM Latency (min)	134.1 (73.6)	76.4 (34.9)**	80.9 (54.9)**	81.4 (39.4)**	8.0	0.0001
SWE (1–4.5Hz; μV^2/Hz x10^4)	5.97 (2.6)	6.47 (2.4)	6.58 (2.3)	8.22 (3.0)***	12.8	<0.0001
First 3.7 Hours of Sleep						
TST (min)	178.7 (34.4)	201.8 (17.6)**	205.4 (21.0)***	206.5 (10.3)***	9.3	<0.0001
WASO (min)	22.9 (23.8)	6.0 (5.1)**	8.3 (17.5)**	8.2 (7.2)**	7.6	0.0002
SE (%)	80.5 (15.5)	90.9 (7.9)**	92.5 (9.5)***	93.0 (4.6)***	9.3	<0.0001
N1 (min)	18.8 (11.5)	10.3 (7.9)**	10.3 (7.7)***	8.5 (5.8)***	9.0	<0.0001
N2 (min)	105.6 (29.7)	107.4 (33.1)	93.7 (23.9)	104.1 (23.2)	1.3	0.28
N3 (min)	37.2 (21.6)	54.3 (23.7)*	59.6 (22.4)***	62.7 (20.0)***	8.3	<0.0001
REM (min)	17.0 (15.1)	29.7 (17.6)**	41.8 (19.3)***	31.2 (16.0)***	10.4	<0.0001
REM Latency (min)	98.7 (34.1)	75.8 (43.8)**	72.1 (37.0)**	81.1 (39.4)	3.7	0.016
SWE (1–4.5Hz; μV^2/Hz x 10^4)	4.11 (2.1)	5.83 (2.2)**	5.66 (2.1)***	5.95 (2.2)***	12.6	<0.0001

BSL, baseline night; SR2, sleep restriction night 2; SR4, sleep restriction night 4; RCV, recovery night; TST, total sleep time; WASO, wake after sleep onset; SE, sleep efficiency (TST/time in bed); SOL, sleep onset latency; N1/2/3, NREM stage 1/2/3 time; REM, stage REM time; REML, REM latency (time from sleep onset to first REM sleep epoch); SWE, global slow wave energy (cumulative power 1–4.5Hz for N2/3 epochs averaged over 173 channels overlying the scalp) reported x10^4. Values are displayed as mean (standard deviation). Degrees of freedom (df) for repeated measures ANOVA for sleep stages and latencies = 3,69 for all comparisons except REM latency during the first 3.7 hours of sleep (=3,62). Differences relative to baseline for sleep restriction and recovery nights denoted by

* ($p<0.05$),

** ($p \leq 0.01$), and

*** ($p \leq 0.001$).

Clin Neurophysiol. Author manuscript; available in PMC 2017 February 01.

Table 2

Global Slow Wave Detection Data.

Full Sleep Episode							
	Parameter	**BSL**	**SR2**	**SR4**	**RCV**	**F- ratio**	**p-value**
All Detected Slow Waves	Amplitude	33.7 (10.8)	37.1 (7.4)	36.9 (6.6)	34.2 (6.2)	3.4	0.022
	Count	5.22 (1.7)	4.99 (1.1)	4.92 (1.2)	6.67 (1.4)**	25.3	<0.0001
	1st Segment Slope	2.69 (1.41)	2.73 (0.57)	2.72 (0.48)	2.55 (0.50)	0.41	0.75
	2nd Segment Slope	1.97 (0.73)	2.04 (0.38)	2.03 (0.34)	1.94 (0.34)	0.54	0.65
High Amplitude Slow Waves	Amplitude	60.5 (14.0)	62.2 (15.8)	58.5 (5.3)	59.1 (5.2)	0.61	0.61
	Count	1.51 (1.0)	1.75 (0.7)	1.78 (0.7)	2.05 (0.8)**	5.2	0.0026
	1st Segment Slope	4.81 (2.39)	4.46 (0.77)	4.30 (0.57)	4.35 (0.52)	0.84	0.48
	2nd Segment Slope	3.21 (1.14)	3.09 (0.67)	2.94 (0.40)	3.03 (0.42)	0.71	0.55
Low Amplitude Slow Waves	Amplitude	22.7 (2.3)	24.6 (1.8)***	24.6 (1.7)***	23.5 (1.8)*	13.8	<0.0001
	Count	3.71 (1.2)	3.25 (1.0)*	3.15 (0.9)**	4.62 (1.3)***	36.2	<0.0001
	1st Segment Slope	1.78 (0.23)	1.89 (0.21)**	1.89 (0.18)*	1.82 (0.21)	5.8	0.0013
	2nd Segment Slope	1.47 (0.19)	1.54 (0.17)*	1.55 (0.15)*	1.49 (0.17)	5.1	0.0030
First 3.7 Hours of Sleep							
All Detected Slow Waves	Amplitude	35.2 (9.1)	38.1 (7.4)	38.0 (7.1)	37.5 (6.9)	2.8	0.046
	Count	3.28 (1.1)	4.32 (0.9)***	4.07 (1.0)***	4.30 (0.9)***	12.6	<0.0001
	1st Segment Slope	2.71 (1.03)	2.78 (0.56)	2.78 (0.51)	2.73 (0.54)	0.18	0.91
	2nd Segment Slope	2.01 (0.56)	2.08 (0.37)	2.08 (0.36)	2.07 (0.37)	0.44	0.72
High Amplitude Slow Waves	Amplitude	59.5 (10.2)	62.1 (16.2)	58.8 (5.6)	59.2 (5.3)	0.64	0.59
	Count	1.08 (0.7)	1.61 (0.6)**	1.55 (0.6)***	1.60 (0.6)***	9.5	<0.0001
	1st Segment Slope	4.56 (1.67)	4.41 (0.73)	4.29 (0.57)	4.26 (0.50)	0.56	0.64
	2nd Segment Slope	3.11 (0.78)	3.08 (0.67)	2.95 (0.41)	3.02 (0.42)	0.43	0.74
Low Amplitude Slow Waves	Amplitude	23.6 (2.2)	25.1 (1.8)**	25.0 (1.7)**	24.8 (1.8)**	7.4	0.0002
	Count	2.20 (0.7)	2.71 (0.8)***	2.51 (0.8)*	2.70 (0.8)***	8.3	<0.0001

Full Sleep Episode							
	Parameter	**BSL**	**SR2**	**SR4**	**RCV**	**F- ratio**	**p-value**
	1st Segment Slope	1.83 (0.23)	1.91 (0.21)*	1.91 (0.18)	1.89 (0.21)	3.07	0.034
	2nd Segment Slope	1.51 (0.18)	1.56 (0.16)	1.57 (0.15)	1.55 (0.17)	2.8	0.046

BSL, baseline night; SR2, sleep restriction night 2; SR4, sleep restriction night 4; RCV, recovery night. High amplitude waves were ≥ 40μV; low amplitude waves were <40μV. Count=number detected slow waves x10^3; Amplitude=mean of peak amplitudes of detected slow waves (μV); 1st and 2nd Segment Slope= amplitude of the most negative peak divided by the time from the previous zero crossing (1st Segment Slope) or the time until the next zero crossing (2nd Segment Slope) in μV/sample. Values are displayed as mean (standard deviation). Degrees of freedom (df) for repeated measures ANOVA for sleep stages and latencies = 3,69.

Differences relative to baseline for sleep restriction and recovery nights denoted by

* ($p<0.05$),

** ($p \leq 0.01$), and

*** ($p \leq 0.001$).